

PAPER • OPEN ACCESS

## Experimental analysis of a CO<sub>2</sub> heat pump for instantaneous domestic hot water production

To cite this article: R Trinchieri *et al* 2020 *J. Phys.: Conf. Ser.* **1599** 012059

View the [article online](#) for updates and enhancements.



**ECS** **240th ECS Meeting**  
Digital Meeting, Oct 10-14, 2021  
**We are going fully digital!**  
Attendees register for free!  
**REGISTER NOW**

# Experimental analysis of a CO<sub>2</sub> heat pump for instantaneous domestic hot water production

R Trinchieri<sup>1</sup>, M Pieve<sup>1</sup>, G Boccardi<sup>1</sup>, N Calabrese<sup>2</sup>, P Rovella<sup>3</sup> and L Saraceno<sup>1</sup>

<sup>1</sup> Energy Dept., Division for Energy Efficient Production, Conversion and Use, Laboratory of Chemical and Thermal Fluid-Dynamic Energy Processes Development, ENEA, C.R.Casaccia - Via Anguillarese, 301 - 00123 Roma (Italy)

<sup>2</sup> Italian National Agency for Energy Efficiency, Energy Efficiency Laboratory in Buildings and Urban Development, ENEA, C.R.Casaccia - Via Anguillarese, 301 - 00123 Roma (Italy)

<sup>3</sup> DIMEG, University of Calabria, via P. Bucci, 87036 Arcavacata di Rende, Cosenza (Italy)

Corresponding author e-mail: maurizio.pieve@enea.it

**Abstract.** The performance of a CO<sub>2</sub> (R744) heat pump (HP) depends strongly on the application and on the environmental operating conditions. In particular, the CO<sub>2</sub> HP becomes competitive compared to traditional heat pumps using halogenated refrigerants in applications characterized by a high hot water demand (hospitals, sport centres, etc.). This paper deals with the experimental analysis of an air-to-water commercial R744 HP tested in ENEA laboratories for instantaneous production of domestic hot water (DHW). The results show that HP efficiency is strongly affected by the inlet water temperature at the gas cooler. A test equipment capable of maintaining the ambient temperature at a desired value (between -10 °C and +20 °C), and managing water flow and water temperature (between 15 °C and 45 °C) is used to evaluate the machine COP as a function of the boundary conditions (inlet gas cooler water temperature, water flow rate, external ambient temperature). The analysis shows the considerable potential of R744 heat pumps for the instantaneous production of DHW, combining a high performance and relevant energy saving. As well, it points out that, to maximize the COP it is necessary to combine the HP with a high stratification storage system, which ensures a suited inlet water temperature, and with a correct value of water flow.

## 1. Introduction

Among the natural fluids, carbon dioxide is one of the most valid alternatives to the use of synthetic refrigerants currently present on the market (mainly hydrofluorocarbons, HFCs) which, although characterized by a very low or zero ODP (Ozone Depletion Potential), often show a too high GWP (Global Warming Potential), thus being not eligible in reducing the greenhouse effect. CO<sub>2</sub> is also one of the few natural fluids neither flammable nor toxic. Moreover, it is compatible with most common mineral oils and does not attack metals or elastomer materials [1, 2]. As for the energy issue, its high compression temperatures may be adequately exploited. For instance, the operating conditions of the gas cooler in a transcritical cycle allow getting high heat exchange performance for DHW production even at very low external ambient temperatures (down to -25 °C).

Some experimental and theoretical studies reported CO<sub>2</sub> HP as a good solution for both residential



and commercial use [3, 4], for refrigeration systems, for space heating and sanitary hot water production [5-7]. In [8] a theoretical analysis is presented of the gas cooler pressure optimisation in the case of fixed water delivery temperature. Unlike that work, this paper presents a larger number of experimental tests with a broader range of thermodynamic parameters. In addition, the influence of many different boundary conditions on the machine COP, in particular the high pressure, is analysed in order to perform an optimized calculation of the performance.

In a transcritical CO<sub>2</sub> system hot water may be produced at relatively high temperature in a counter-current flow with the hot refrigerant at the compressor outlet, showing very high heat transfer efficiency. Unlike traditional fluids used for heat pumps, the temperature profiles of carbon dioxide (e.g., at a pressure of 120 bar with cooling from 100 °C to 20 °C approximately) and water (being heated from 15 °C up to 90 °C) appear to be very close and with similar trend. The high temperature levels allow to get an optimum matching with the stratified storage tanks. Indeed, high temperatures permit to store large amounts of energy, thus producing hot water during the night hours, while energy loads are lower and tariffs may be more convenient. A further advantage of such high temperature system is the intrinsic avoidance of bacteria development (for instance the legionella). With a high stratification accumulation system, the achievement of HP high efficiencies is feasible since the CO<sub>2</sub> transcritical cycle efficiency is strongly linked to the gas cooler inlet water temperature and it increases while the latter is decreasing [5, 9].

Due to the CO<sub>2</sub> characteristics, the HP equipment may be very compact, allowing a considerable reduction of the space required. On the other hand, high operating pressures require the use of a robust circuit, compliant with the specific safety standards.

The aim of the experimental campaign was to assess the HP performances while varying the boundary conditions and to verify the limits for the instantaneous production of DHW. The tests were performed at different ambient temperatures, with many water flow rates and inlet water temperatures. The refrigerant flow was managed as well, keeping it within the limits of the compressor running parameters, by acting on the set points of the machine and, in some tests, on the control and management system of the electronic lamination valve.

A first series of tests was conducted keeping constant both the ambient temperature and the water temperature; in a second series the ambient temperature only was varied. Finally, other tests were carried out by varying both the environmental temperature and the inlet water temperature. First tests showed the influence of compressor and gas cooler performances on the overall performance, while the second series of tests showed the influence of evaporator working conditions on the heat pump performances. Finally, the third series allowed to calculate the performance decrease due to the increase of the gas cooler inlet water temperature. All experimental results were used to verify the limits in the production of DHW in instantaneous way. As for the latter issue, the maximum producible water flow rate was evaluated in instantaneous mode, without any storage system.

## 2. Experimental

For the experimental campaign a 4.5 kW heating capacity commercial R744 heat pump was used for producing sanitary hot water. In its standard mode, the hot water produced is stored in a storage tank, to be subsequently used both for space heating and for DHW supply on-demand.

### 2.1. Materials and methods

The heat pump "heart" is certainly a two-stage rotary CO<sub>2</sub> compressor, capable of bearing high pressure differences, subject to very small losses and characterized by a low level of vibrations. The compressor has reduced noise level as well and its compact and lightweight design allows a substantial size and weight reduction of the heat pump.

The water heat exchanger acts as a gas cooler and it is a tube-in-tube heat exchanger with a particular design developed by SANYO, providing heat transfer efficiency increase of about 60% compared to traditional solutions.

The expansion device is the JKV14 version of the Electronic Expansion Valve Saginomiya,

specifically designed for carbon dioxide applications. The valve opening degree is usually managed by the control system of the machine, which processes the operating temperatures measured by dedicated probes installed in the CO<sub>2</sub> circuit. During laboratory activities, an external control system was installed, used in some tests, based on an ARDUINO module, allowing the transmission of an appropriate signal sequence for valve opening or closing, independent from the CO<sub>2</sub> temperatures in the circuit.

The evaporator is a finned coil heat exchanger coupled to an axial fan for forced convection heat transfer between the refrigerant fluid and the air. Special care in the design of the refrigerant circuit ensures an effective frost protection system for the lower zones of the heat exchanger, thus avoiding the use of electric heaters or cycle inversion. In practice, the defrost system is achieved by directing the hot gas coming out from the compressor to the lower part of the evaporator (thus before entering the expansion valve), so that the evaporator wall temperature is kept above 0 °C. Figure 1 depicts all the components.

## 2.2. Transducers and sensors

The heat pump is equipped with K- and J-type thermocouples and pressure transducers to monitor the CO<sub>2</sub> thermodynamic states at the ends of each component. The measuring points are shown in figure 1.

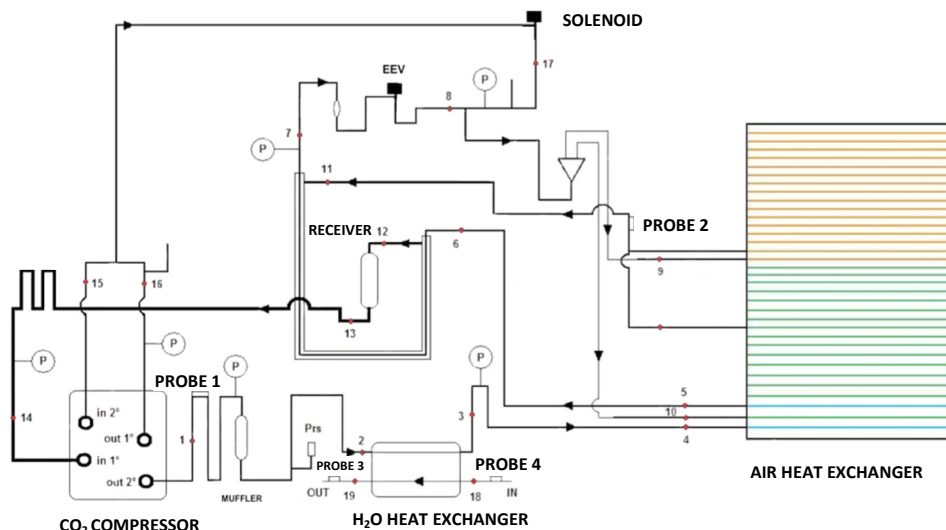


**Figure 1.** Heat pump system layout with instruments and measuring points.

The refrigerant cycle is depicted on Temperature-Enthalpy plot and consists of the following processes (figure 2):

- compression (points 14-16, first stage compression, 16-1, second stage compression);
- CO<sub>2</sub> cooling in the gas cooler (2-3). In this component the water heating occurs as well.
- CO<sub>2</sub> subcooling in the regenerative heat exchanger (6-7);
- expansion in the electronic expansion valve (EEV, 7-8);
- CO<sub>2</sub> evaporation and superheating, with the main flow split in two different streams (8-12);
- A hot-gas defrost system is provided if necessary, driven by a special solenoid valve (17);
- Another defrost system is provided as well for the lower section of the evaporator, by means of the CO<sub>2</sub> exiting the gas cooler (4-5).

Two Coriolis flow meters are also added to measure the mass flow rate of CO<sub>2</sub> and water into the gas cooler. The carbon dioxide flow meter is added at the outlet of the second compressor stage. The output signals of pressure transducers, flow meter sensors and electrical power sensor are 4-20 mA current signals proportional to the measured values, and they are sent to the data acquisition system,

managed by NI LabVIEW software. The CO<sub>2</sub> thermodynamic parameters (e.g. enthalpy, entropy, specific heat, etc.) are calculated according to pressure and temperature measures with REFPROP software [10]. Finally, the measures are used to evaluate COP, heat capacity at gas cooler side, gas cooler effectiveness and compressor efficiency.

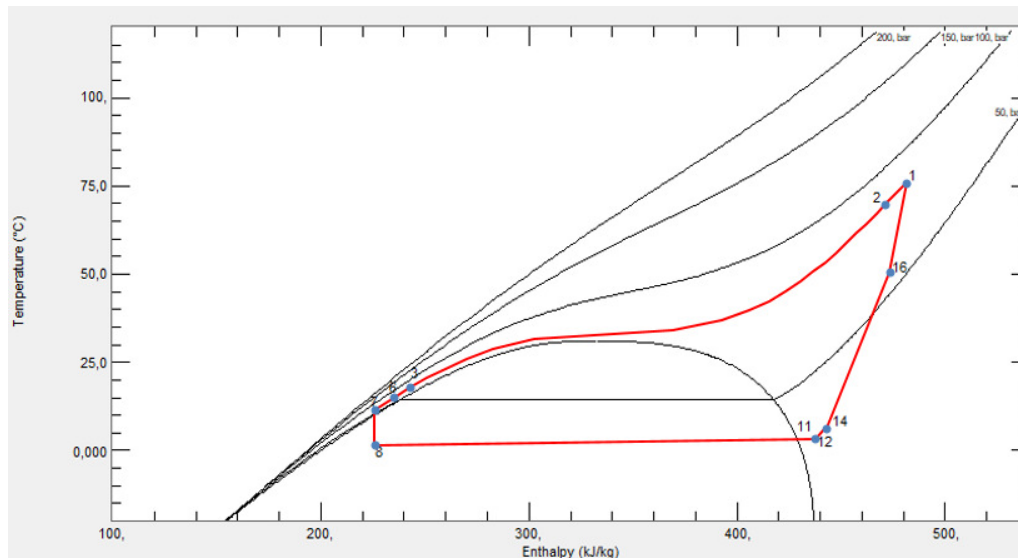


Figure 2. R744 Temperature-Enthalpy plot with measuring points.

### 3. Theoretical analysis

The heat pump performance is measured by COP (Coefficient Of Performance), calculated as follows:

$$COP = \frac{G_{CO_2}(h_{inGC} - h_{outGC})}{W_{el}} \quad (1)$$

where  $h_{inGC}$  and  $h_{outGC}$  are the CO<sub>2</sub> enthalpy at gas cooler inlet and outlet, respectively,  $G_{CO_2}$  is the carbon dioxide flow rate, and  $W_{el}$  is the total electric power consumption.

The overall efficiency of the compressor is defined according to the following relationship:

$$\eta_g = \frac{G_{CO_2}(h_{outCPis} - h_{inCP})}{W_{CP}} \quad (2)$$

where  $h_{outCPis}$  is CO<sub>2</sub> enthalpy at the compressor outlet evaluated with isentropic conditions respect to the compressor input,  $h_{inCP}$  is the CO<sub>2</sub> enthalpy at compressor inlet, and  $W_{CP}$  is the electrical absorbed power of the compressor.

The heat exchanger effectiveness  $\varepsilon$  indicates the heat transferred in a heat exchanger with respect to the maximum possible one. This latter, according to the Second Law of Thermodynamics, would be theoretically obtained when the outlet temperature of the fluid with the lowest hourly heat capacity rate  $C$  ( $C = m \cdot c_p$ ) is equal to the inlet temperature of the other fluid, by means of a practically infinite size counter-current flow heat exchanger. In our test conditions, however, a unique fluid with a capacity rate lower than the other does not exist, since the CO<sub>2</sub> specific heat capacity undergoes a very high and sharp variation during the gas cooling process. Indeed, under certain conditions, depending on CO<sub>2</sub> pressure and on the mass flow rate ratio  $G_{water}/G_{CO_2}$ , it may happen that the maximum heat transferrable does not mean a matching between the temperatures at the end of the gas cooler, but a pinch point occurs inside the heat exchanger, which corresponds to the actual upper limit of transferrable heat between the two flow streams. Chen [11] illustrates how to determine the maximum possible heat transfer rate, when the

curves of water and CO<sub>2</sub> are tangent, so that the gas cooler effectiveness may be calculated.

#### 4. Results and discussion

The tests were executed with HP in stationary conditions, achieved after the initial transient period.

In order to maintain the desired temperature conditions in the ambient surrounding the heat pump, a climatic chamber is used: in so that, using the cold flow available from the machine itself, some tests were executed at ambient temperatures down to about -10 °C. Table 1 reports the ranges of temperature, pressure, flow and electric power consumption recorded during of all the tests. The sensors were included in table 1 too, their position being as figure 1 shows.

**Table 1.** Minimum and maximum values of the acquired parameters in tests.

	Temperature (°C)			Water flow (kg/h)	Electric power (kW)	Pressure (bar)		Env. T (°C)	CO2 flow rate (kg/h)	COP
<b>Position</b>	2	18	8	-	-	1	14	-	-	-
<b>Min</b>	56.4	15.1	-17.4	92.5	0.98	69.2	18.1	-9.51	53.03	0.76
<b>Max</b>	115.7	48.1	21.6	337.5	2.27	121.7	57.3	23.32	119.8	4.85

Table 2 lists the instrument specifications and their uncertainty, as indicated by the manufactures.

**Table 2.** Measurement instrumentation and calibrated uncertainties.

Measurement	Range/Unit	Uncertainty
Temperature (K-type)	0/150 °C	± 1.1 K
Temperature (J-type)	-40/80 °C	± 1.1 K
Pressure	0-60/0-100/0-160 bar	0.08%
Water flow rate	0/200 l/min	0.02% of reading
Electrical power	0/25 kW	Precision class 0.5
CO <sub>2</sub> mass flow meter	0/0.95 kg/s	± 0.10% of reading

When the control was made by acting with the external controller on the closure degree of the EEV, the performance of the machine was not in line with the other tests.

By analysing the experimental data the machine overall performance was evaluated, as well as the effects of different boundary conditions on the operating efficiencies of the individual components, in particular the gas cooler and the compressor; in the following, correlations are presented for each test between the characteristic parameters averaged over steady working period of the HP. As for the compressor performance, the experimental results show that it ensures high performances in any operation conditions.

Figure 3 shows the overall efficiency of the compressor, defined according to the equation (2), with  $\eta_g$  values between 0.67 and 0.75 (shown as a function of the compression ratio,  $\beta$ ), thus being widely acceptable even with the worst boundary conditions (very low ambient temperatures).

The analysis of the other components performance is done by dividing the experimental tests in three groups. The first group were carried out with constant air temperature at the evaporator (equal to 19 °C) and constant inlet water temperature of 16 °C. The second group includes tests with air temperature in the range -9 °C ÷ 14 °C and inlet water temperature still fixed at 16 °C. In the third series of tests, both the air temperature at the evaporator and the feed water temperature were varied. The latter was varied between 16 °C and 50 °C, in order to evaluate the machine performance trend as a function of this parameter and to verify the water mass flow limits for DHW instantaneous production.

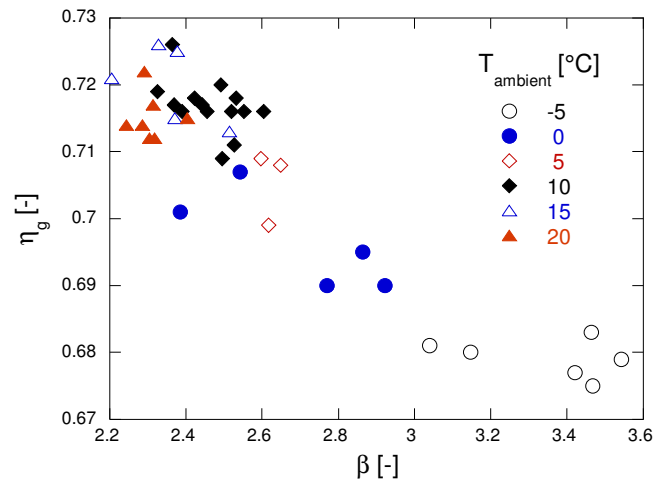


**Figure 3.** Compressor global efficiency  $\eta_g$  vs the compression ratio  $\beta$ .

*4.1. Tests with constant air temperature and constant water temperature at gas cooler inlet*

The tests were carried out varying the water flow rate at the gas cooler inlet,  $G_{water}$ , and operating under fixed conditions for ambient ( $T_{amb} \approx 19 \text{ }^\circ\text{C}$ ) and water temperature ( $T_{water\_inGC} = 16 \text{ }^\circ\text{C}$ ), and refrigerant flow rate. In this series of tests the evaporator working conditions may be assumed substantially constant.

As expected, the water temperature at the gas cooler outlet decreases as the water flow increases, as shown in figure 4 and a certain influence of the discharge cycle pressure on the temperature obtained at the same flow rate (for example 130 kg/h) can be noted. As for the heat pump performance, the COP is plotted as a function of the water flow rate in figure 5 and it is shown to increase up to about 4.5, with an overall increase of about 25%. The lowest measured values of COP are mainly due to the gas cooler decreased effectiveness with low water flow, as shown in figure 6, where the COP is plotted as a function of the gas cooler effectiveness. The latter is calculated according to [11], and assuming an isobaric cooling of  $\text{CO}_2$  for the ideal condition of maximum transferrable heat. It shows that, when water flow rate is higher than 150÷200 kg/h the gas cooler effectiveness approaches its theoretical maximum (i.e. unity) and the COP increases with the water flow.

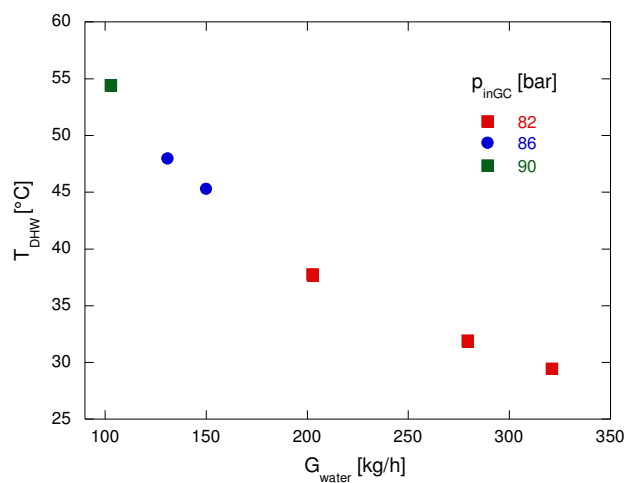


**Figure 4.** Water outlet temperature vs water flow rate.

This outcome is fully consistent with the gas cooler analysis made by Chen [11], since the mass flow ratio between the water and the refrigerant is slightly greater than 2. It should be recalled, in this regard,

that a unitary effectiveness means that the pinch point is located at the cold end of the gas cooler, and the water and the CO<sub>2</sub> have virtually the same temperature.

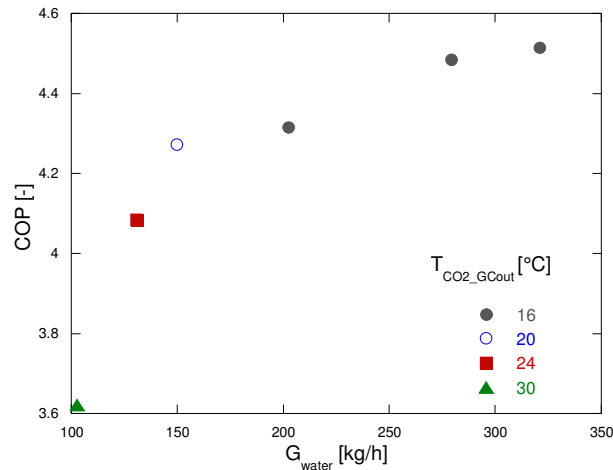


**Figure 5.** Heat pump COP vs water flow rate.

Figure 7, where the COP is plotted as a function of the temperature difference on gas cooler cold side, shows that the CO<sub>2</sub> gas cooler outlet temperature tends to increase when the water flow rate decreases: for instance, at a flow rate of 100 kg/h, the temperature difference between the outgoing CO<sub>2</sub> and the incoming water is about 14 °C, while for higher flow rate such difference is progressively reduced down to 0 (close to 100% effectiveness). The thermodynamic reason for the heat exchanger effectiveness reduction when varying the water flow rate can be explained by comparing figures 8 and 9, where temperature profiles at the gas cooler with different water flow rates are shown in a T-Q diagram. They were calculated by means of the available experimental data and a 100-step discretization model of the gas cooler, assuming a counter-current flow arrangement, and applying the energy balance to each section. The continuous lines represent the CO<sub>2</sub> temperature trend, while the dashed lines represent the water temperature in the same heat exchanger section (temperature profiles could also be analyzed according to T-S diagram like Neksa et al. [12]).

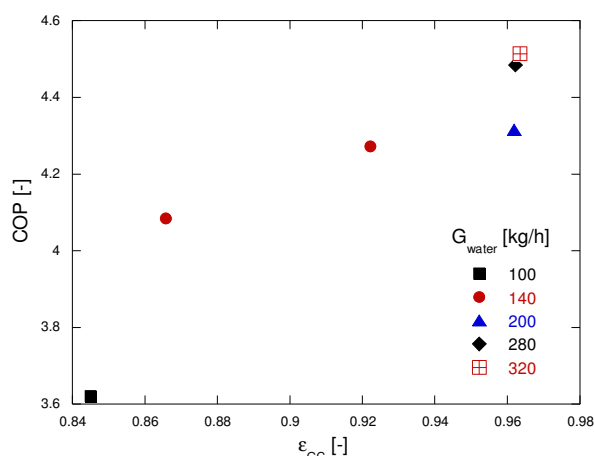


**Figure 6.** Heat pump COP vs gas cooler effectiveness.

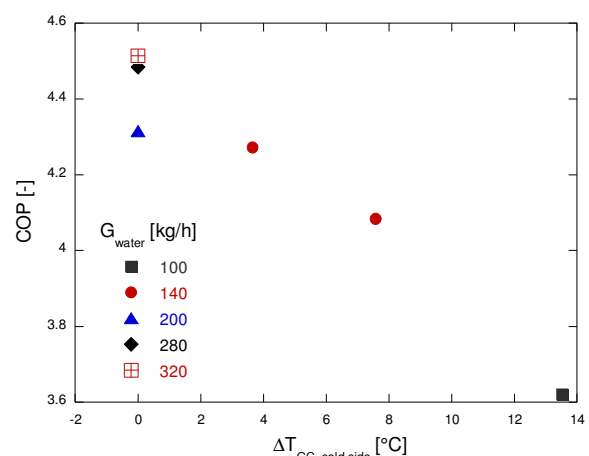


**Figure 7.** Heat pump COP vs  $\Delta T$  on gas cooler cold side.

When the water flow is low (100 kg/h,  $G_{\text{water}}/G_{\text{CO}_2} = 1.11$ ), the water temperature variation is larger, i.e. the slope of the dashed line in figure 8 is greater than that corresponding in figure 9. This causes the



pinch point to fall inside the heat exchanger, thus making impossible to obtain a small temperature difference at the cold end. Moreover, the pressure drop occurring in the heat exchanger ranges about 7÷10 bar, thus the problem of a mismatch between the two curves worsens. Incidentally, such a high pressure drop, being an important source of irreversibility in the cycle, should be further investigated.

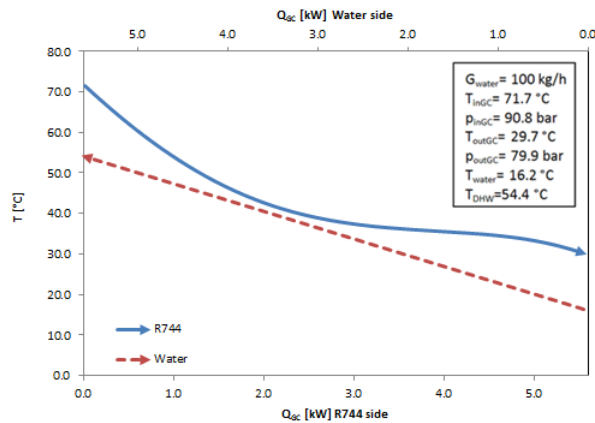


**Figure 8.** Water and CO<sub>2</sub> temperature profiles vs heating capacity -  $G_{\text{water}} = 100 \text{ kg/h}$ .

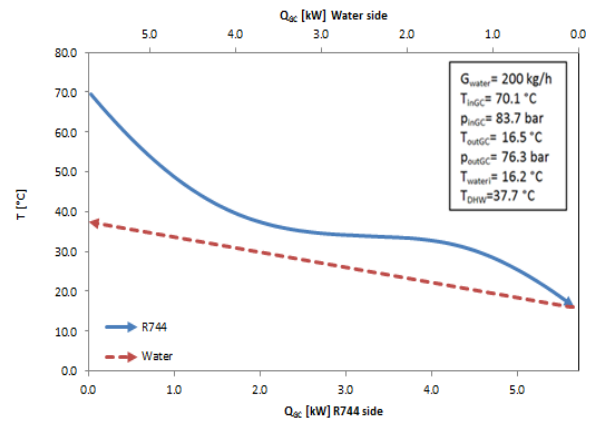


**Figure 9.** Water and CO<sub>2</sub> temperature profiles vs heating capacity -  $G_{\text{water}} = 200 \text{ kg/h}$ .

The comparison between the two figures clarifies how much the water flow rate can get the instantaneous DHW production an efficient process, provided that the machine is operated at an optimal gas cooler discharge pressure. Therefore, a HP control should be assured that is able to establish the correct value of cycle high pressure depending on the boundary conditions.

#### 4.2. Tests with variable air temperature and constant water temperature at gas cooler inlet

Figure 10 shows the water outlet temperatures obtained as a function of the water flow rates. With flow rates between 100 and 150 kg/h, water temperatures are obtained around 50 °C. With these water flow rates, gas cooler effectiveness is reduced down to 25%, compared to the maximum achievable. For a fixed flow rate, the effectiveness depends on the gas cooler pressure: this occurs when the gas cooler pressure is very low, lower than optimal value, and is not determined by the heat transfer because CO<sub>2</sub> operates in transcritical conditions [12]. Such effect therefore confirms the strong influence of the gas cooler discharge pressure on the optimal set of parameters for R744 HPs use [2, 7, 13].

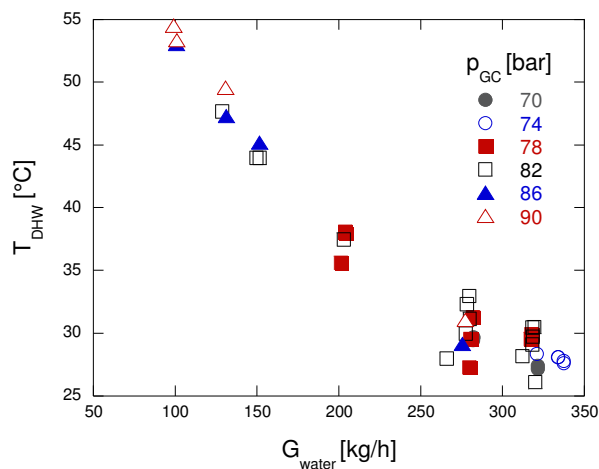


**Figure 10.** Water outlet temperature vs water flow rate.

The experimental results show that COP depends both on  $G_{\text{water}}$  and  $T_{\text{amb}}$  (Figure 11). With low water

flow rates the observed reduction in COP may be also attributed to the gas cooler effectiveness reduction. With water flow rates greater than 200 kg/h, the COP decrease at ambient temperatures lower than 5 °C may be due to the evaporator working conditions. Figure 12, where COP is plotted versus evaporation temperature, shows that the COP is substantially proportional to the evaporation temperature until the gas cooler effectiveness is high enough, since the evaporation temperature,  $T_{ev}$ , and the corresponding evaporation pressure,  $p_{ev}$ , decrease when ambient temperature decrease, resulting in  $\beta$  increase and deterioration of the compressor overall performance (shown in figure 3).

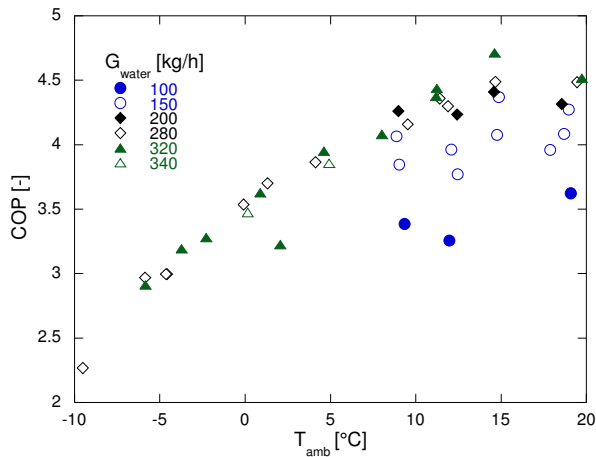


Figure 11. COP vs ambient temperature.

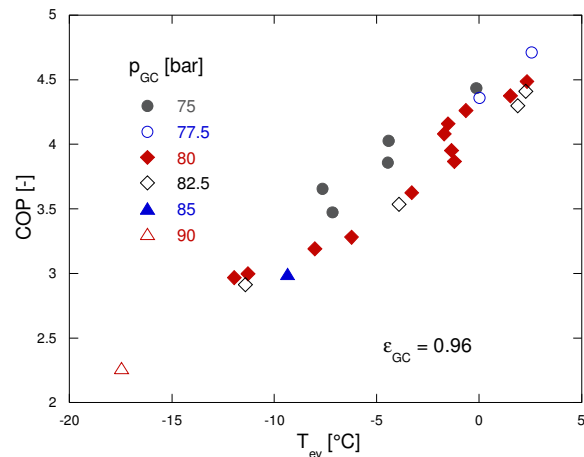


Figure 12. COP vs evaporation temperature.

#### 4.3. Tests with variable air temperature and variable water temperature at gas cooler inlet

This series of tests allowed to identify the influence of the gas cooler inlet water temperature ( $T_{water\_inGC}$ ) on the heat pump performances. Figure 13, where COP is plotted as a function of the inlet water temperature, shows a considerable influence on COP reduction, which reaches values around unity when the water temperature approaches 45 °C. The effect of the ambient temperature,  $T_{amb}$ , is less important, especially when  $T_{water\_inGC}$  approaches and exceeds 35 °C. Indeed, for high  $T_{water\_inGC}$  there are no substantial COP variations with  $T_{amb}$ , while reducing  $T_{water\_inGC}$  (for example when this is equal to 20 °C or 24 °C), COP increases with  $T_{amb}$ , as already shown in figure 11. This is strictly linked to the relation between  $T_{water\_inGC}$  and the CO<sub>2</sub> critical temperature. Different COP values of tests with the same values of  $T_{water\_inGC}$  and  $T_{amb}$  are due to the different water flow rates of each test.

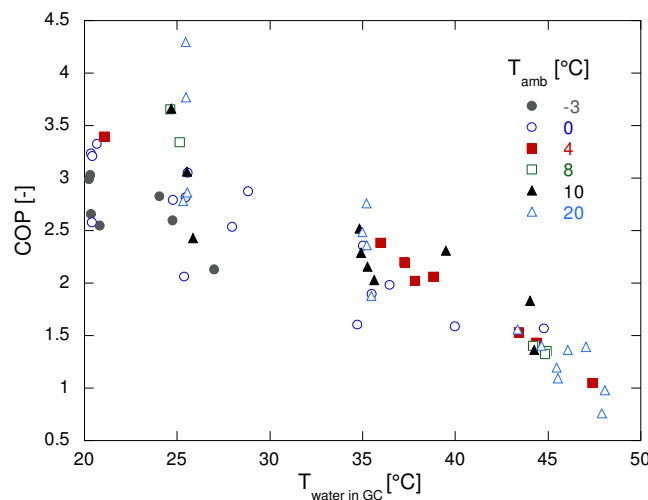


Figure 13. COP vs water inlet temperature.

When similar water flow rates and ambient temperatures (200 kg/h and 10 °C, respectively) are considered,  $T_{\text{water\_inGC}}$  influences, as expectable, the amount of CO<sub>2</sub> cooling at the gas cooler. A comparison was made between two tests, where  $T_{\text{water\_inGC}}$  was equal to 25 °C and 45 °C respectively. From a cycle standpoint, the lower water temperature at the gas cooler inlet causes a cycle enlargement, so that enthalpy, temperature and quality at the evaporator inlet are lower than the other case: in this way, the evaporator can provide a larger heat extraction capacity which can be transferred to the water at the gas cooler. It is noteworthy that under these conditions (CO<sub>2</sub> temperature at gas cooler outlet of 25 °C), acting on the discharge pressure is less important and less effective than the other case, due to the almost vertical slope of the corresponding isotherm at the gas cooler outlet. In the other case (CO<sub>2</sub> temperature at gas cooler outlet of 45 °C), increasing the gas cooler pressure could determine a significant increase of the enthalpy available at the evaporator and the gas cooler and, consequently, of the COP (fixed  $W_{e1}$ ): this would occur because of the milder slope of isotherms at temperatures higher than 35 °C [14].

Moreover, according to the tests, the pressure drop at the gas cooler is responsible for a significant deterioration of the performances, more pronounced in case of high water temperatures at the gas cooler outlet. In order to evaluate the importance of working with optimized discharge pressures ( $p_{GC}$ ) and the corresponding achievable COP improvements, a simple ideal CO<sub>2</sub> refrigeration cycle with a spreadsheet was simulated, calculating optimal values of  $p_{GC}$  as a function of outlet gas cooler water temperature ( $T_{\text{CO}_2\text{\_outGC}}$ ) [15]. Figure 14, where COP is plotted as a function of gas cooler pressure (no pressure loss effect was considered), refers to a simulation with evaporation temperature  $T_{ev}$  fixed at 0 °C,  $\Delta T_{sur}$  (superheating) equal to 5 °C and compressor efficiency  $\eta_g$  equal to 0.7: the results show how much the choice of the suited  $p_{GC}$  allows a substantial COP increase, once fixed  $T_{\text{CO}_2\text{\_outGC}}$ .

A simulation done by fixing  $T_{ev}$ ,  $\Delta T_{sur}$  and  $\eta_g$  equal to the experimental values, gave, for each test, the optimum gas cooler pressure ( $p_{GCopt}$ ) and the corresponding ideal obtainable COP.

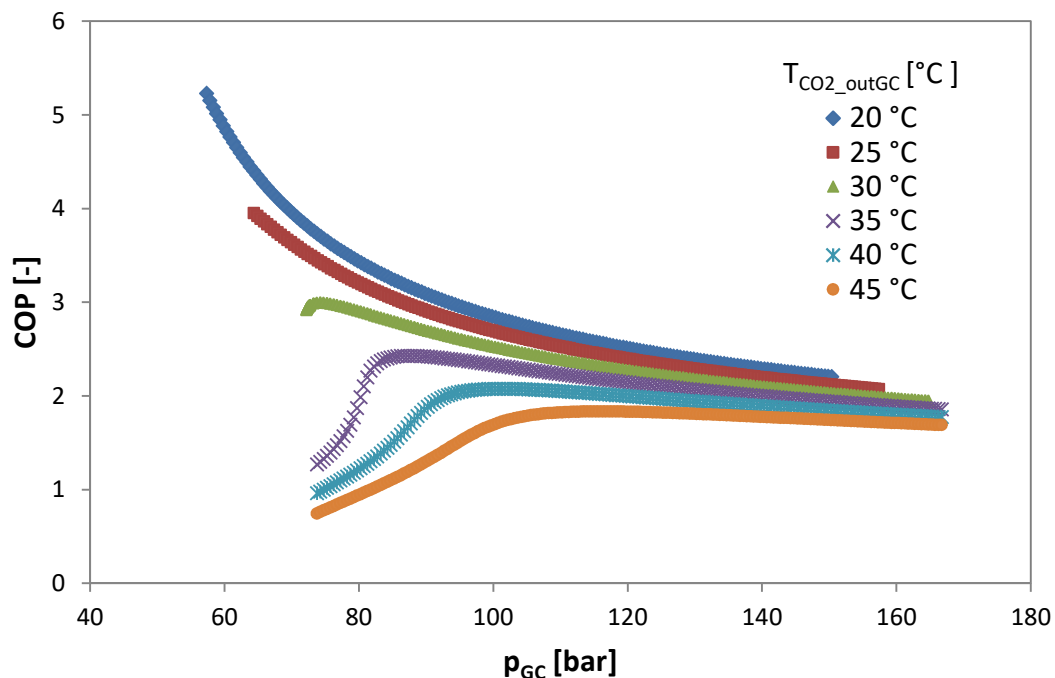


Figure 14. COP vs gas cooler pressure ( $T_{ev} = 0$  °C).

The ideally achievable COP at the optimum pressure, indicated as  $COP_{p_{GCopt}}$ , may be compared with COP obtained in the experimental tests,  $COP_{p_{GC}}$ . A simulation cycle was assumed without the contribution of the air-CO<sub>2</sub> heat exchanger after the gas cooler. As a result of the simulation, a parameter was obtained which measures the difference, named  $\Delta COP_{pc}$ :

$$\Delta\text{COP}_{pc} = \frac{(\text{COP}_{p_{GC}} - \text{COP}_{p_{GCopt}})}{\text{COP}_{p_{GCopt}}} \quad (3)$$

More precisely,  $\Delta\text{COP}_{pc}$  provides, for each test, the percentage deviation of the experimental COP compared to the optimum COP obtained in a simulation where  $p_{GCopt}$  is calculated with experimental  $T_{ev}$ ,  $\Delta T_{sur}$  and  $\eta_g$ . Figure 15 presents a comparison between the experimental pressure and the optimum pressure parameterized according to  $\Delta\text{COP}_{pc}$ . The points on the left side of the plot refer to tests whose  $p_{GC}$  are higher than  $p_{GCopt}$ , while those on the right have lower values. As far the discharge pressure deviation from the optimum value is positive and lower than 10%, (tests at the left of the bisector within the +10% line) a COP reduction results lower than 15%, as indicated by the parameter  $\Delta\text{COP}_{pc}$  in figure 15, according to the expectations. If the pressure deviation is greater than 10% compared to the optimum value, COP decrease to 65% may be experienced.

When the discharge pressure is lower than the optimum, even though very close to  $p_{GCopt}$  (points in figure 15 on the right of the bisector within the -10% line),  $\text{COP}_{p_{GC}}$  shows values very lower than  $\text{COP}_{p_{GCopt}}$ , even by 35-45%.

The reason for this trend may be found in the analysis reported in figure 16, where  $p_{GC}$  is plotted versus  $p_{GCopt}$  again with a different parameter. It shows that almost all the tests belonging to this band are characterized by  $T_{CO_2, outGC}$  between 30 °C and 40 °C. In such cases, (see the corresponding curves in figure 14) when the discharge pressure is slightly lower than optimal value, COP considerably decreases. Therefore, in these cases it is advisable to work at pressures higher than the optimum, consistently to some technical literature results on the same issue [16-17].

Looking at figure 15, the tested heat pump shows an internal regulation such that  $p_{GC}$  varies in a quite narrow range during variable testing conditions, i.e. between about 65 and 95 bar, while the optimum pressure should vary between 40 and 110 bar. Comparing figures 15 and 16 with the plots of figure 14 it can be affirmed that, when the machine operates with  $T_{CO_2, outGC}$  between 15 °C and 25 °C, a too high  $p_{GC}$  would cause a considerable COP reduction due to high slope of the curve ( $\text{COP}-p_{GC}$ ). On the other hand, it should be highlighted that, for the needed  $T_{CO_2, outGC}$ , setting the pressure at the optimal value is not always desirable or possible, since the gas cooler  $CO_2$  inlet temperature would be too low for the DHW production. Moreover, the pressure at the gas cooler depends also on the compressor size and the amount of charge in the refrigerant loop, so that, once these latter are fixed, it would not be possible to reduce the pressure to the optimal values.

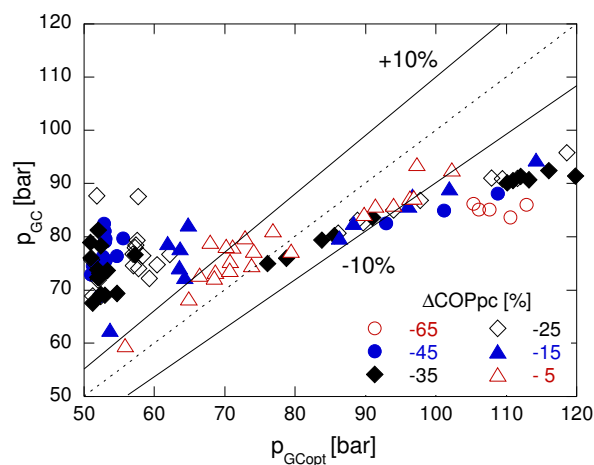


Figure 15.  $p_{GC}$  vs  $p_{GCopt}$  (parameter  $\Delta\text{COP}_{pc}$ ).

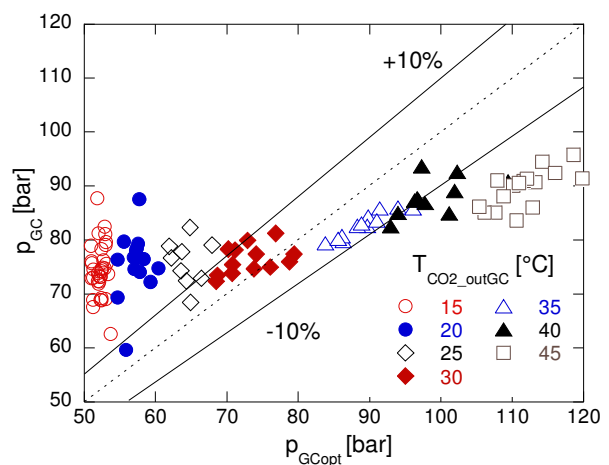


Figure 16.  $p_{GC}$  vs  $p_{GCopt}$  (parameter  $T_{CO_2, outGC}$ ).

As for the tests with  $p_{GC}$  lower than 10% compared to the optimum (i.e., practically the tests having  $T_{CO_2, outGC}$  higher than 40 °C in figure 16), it should be noted that the optimum pressure significantly exceeds 100 bar and, in this case, considerations about the machine reliability would recommend to

operate at lower pressures. Incidentally, the tested heat pump operates at these pressure levels during the defrosting phase in the evaporator.

The heat pump working pressure (average value around 80 bar, as shown in figures 15 and 16) is maintained around the optimal value with  $T_{\text{water\_in\_GC}}$  between 30 °C and 35 °C, based on the compressor size, the refrigerant charge and the adjustment and control system of the expansion valve opening.

These considerations may lead to conclude that, if a cold constant temperature thermal sink is available to cool the CO<sub>2</sub> in the gas cooler and the refrigerant circuit and its components are accordingly sized, the heat pump may operate with COP very close to the optimum values, irrespective of the other boundary conditions, such as the ambient temperature.

About this, the combination of a CO<sub>2</sub> heat pump system with a high stratification storage tank is crucial to stabilize the cooling water temperature, while ensuring that the heat pump operates always with high performance [8].

## 5. Conclusions

The experimental campaign described in the paper was done with the main aim of providing an evaluation of the DHW production capability by means of a CO<sub>2</sub> heat pump in instantaneous way. Although the tested machine has a small capacity (4.5 kW heating capacity), and therefore it is not able to produce the amount required by the current regulations (UNI EN 806-4:2010), the experimental tests allowed to highlight many issues:

- the compression process of CO<sub>2</sub> can be conducted with high efficiencies through the use of advanced two-stage compressors;
- the gas cooler is a rather important component, in order to get high COP values. Once the domestic hot water flow rate and its final temperature are fixed, the CO<sub>2</sub> working pressure has to be correctly evaluated to obtain high effectiveness; for this purpose, it is essential to design a heat exchanger with as small as possible pressure drop, as well ensuring high heat transfer performance;
- according to the concepts above stated, the importance of the heat pump control and management system is significant; for example, it allows the optimization of the discharge pressure with boundary varying conditions by means of an inverter for the compressor;
- an evaporator as more efficient as possible is needed in order to improve the compressor operating conditions.

The gas cooler optimal pressure evaluation, obtained by means of a simple numerical simulation, showed that the tested heat pump is designed to operate with COP close to the optimal COP when the cooling water temperature is close to 30 °C ÷ 35 °C, regardless of the ambient temperature.

This outcome may lead to conclude that the combination of the CO<sub>2</sub> heat pump with a high stratification storage system, capable to feed the heat pump with an almost constant temperature would allow the heat pump operation with high COP. Indeed, if the sink temperature is known, the sizing of all the heat pump components would be possible depending on the corresponding optimal pressure, in order to get it works close to the maximum achievable COP, accordingly to the specific application.

As for the HP capability of instantaneous DHW production with high COP and without a high stratification storage system, the heat pump showed to require higher water flow rates, as well as to operate with low CO<sub>2</sub> temperature at gas cooler outlet and an adaptive control logic able to establish the correct value of the discharge pressure according to the boundary conditions. In conclusion, the present study, despite the small size of the tested machine, shows good perspectives for the development of dedicated CO<sub>2</sub> heat pumps for the instantaneous DHW production, especially when they are combined with high stratification storage systems.

## References

- [1] Cavallini A 2004 *Proc. European Seminar Carbon Dioxide as a refrigerant (Milan)*
- [2] Kim M H, Pettersen J and Bullard C W 2004 *Prog. Energ. Combust.* **30** (2) 119-74

- [3] Boccardi G, Calabrese N, Celata G P, Mastrullo R, Mauro A W, Perrone A and Trinchieri R 2013 *Appl. Therm. Eng.* **54** 528-35
- [4] Girotto S, Minetto S and Neksa P 2004 *Int. J. Refrig.* **27** 717-23
- [5] Cecchinato L, Corradi M, Fornasieri E and Zamboni L 2005 *Int. J. Refrig.* **28** 1250-8
- [6] Lorentzen G 1994 *Int. J. Refrig.* **17** (5) 292-301
- [7] Neksa P 2002 *Int. J. Refrig.* **25** 421-7
- [8] Minetto S 2011 *Int. J. Refrig.* **34** 742-51
- [9] Rieberer R, Kasper G and Halozan J 1997 *Proc. IEA-IIR Workshop CO2 technology in Refrigeration, Heat Pumps & Air Conditioning Systems (Trondheim)*
- [10] Lemmon E W, Huber M L and McLinden M O 2010 NIST Standard Reference Database 23, Version 9.0
- [11] Chen Y 2016 *Int. J. Refrig.* **69** 136-46
- [12] Neksa P, Rekstad H, Reza Zakeri G and Schiefloe P A 1998 *Int. J. Refrig.* **21** (3) 172-9
- [13] Casson V, Cecchinato L, Corradi M, Fornasieri E, Girotto S, Minetto, Zamboni L and Zilio C 2003 *Int. J. Refrig.* **26** 926-35
- [14] Kauf F 1999 *Int. J. Therm. Sci.* **38** 325-30
- [15] Zhang X P, Fan X W, Wang F K and Shen H G 2010 *Appl. Therm. Eng.* **30** 2537-44
- [16] Cecchinato L, Corradi M and Minetto S 2010 *Appl. Therm. Eng.* **30** 1812-23
- [17] Yang L, Li H, Cai S, Shao L and Zhang S 2015 *Appl. Therm. Eng.* **89** 656-62